— **Regular Article** —

Induction of Inflammatory Responses in Mice Treated with Cerium Oxide Nanoparticles by Intratracheal Instillation

Eun-Jung Park,[a] Wan-Seob Cho,[b] Jayoung Jeong,[b] Jong-heop Yi,[c] Kyunghee Choi,[d] Younghun Kim,[e] and Kwangsik Park*,[a]

[a]College of Pharmacy, Dongduk Women's University, 23–1 Wolgok-dong, Seongbuk-gu, Seoul 136–714, Republic of Korea, [b]Division of Toxicological Research, National Institute of Toxicological Research, 38–29, Nokbeon-dong, Eunpyung-gu, Seoul 122–704, Republic of Korea, [c]School of Chemical and Biological Engineering, Seoul National University, 599 Gwanangno, Gwanak-gu, Seoul 151–742, Republic of Korea, [d]Department of Chemical Assessment, National Institute of Environmental Research, Gyeongseo-dong, Seo-gu, Incheon 404–170, Republic of Korea and [e]Department of Chemical Engineering, Kwangwoon University, 447–1 Wolgye-dong, Nowon-gu, Seoul 139–701, Republic of Korea.

(Received May 27, 2009; Accepted January 25, 2010)

Cerium oxide nanoparticles have a high thermodynamic affinity for oxygen and sulfur, which makes them useful in applications such as catalysts, solar cells, and gas sensors. In this study, we investigated the effects of intratracheal instillation of cerium oxide nanoparticles on the inflammatory responses in mice. The number of neutrophils in bronchoaveolar lavage (BAL) fluids was significantly elevated on day 1 after instillation. Inflammatory cytokines, such as interleukin (IL)-1, tumor necrosis factor (TNF)-α, and IL-6, were also increased in BAL fluid and the cytokine increase initiated the differentiation of naive T cells, followed by the induction of Th1-type cytokines [IL-12 and interferon (IFN)-γ] and Th2-type cytokines (IL-4, IL-5, and IL-10). The secretion of Th1-type cytokines was more dominant than that of Th2-type cytokines. The inflammatory responses were maintained for 28 days by a positive feedback stimulation of IFN-γ and IL-10. In the lung, the expression of inflammatory genes was increased in a time-dependent manner, and granuloma formation appeared on day 14 after instillation. This suggests that intratracheal instillation of cerium oxide nanoparticles causes a delayed-type hypersensitivity reaction and lung fibrosis in mice.

Key words —— cerium oxide nanoparticle, intratracheal instillation, inflammation, mice

INTRODUCTION

With the development of nanotechnology, research related to the hazards of nanomaterials has been increasing rapidly. Nanomaterials released into the environment, through natural or artificial processes, enter the human body primarily through the respiratory pathway. However, the respiratory effects of the nanoparticles commonly used in industry have not been fully studied; therefore their potential for hazardous effects on human health remain unclear. As a lanthanide element, cerium oxide nanoparticles are nanomaterials with a wide range of applications, including use as catalysts, in solar cells, fuel cells, gas sensors, and oxygen pumps, and in metallurgical and glass/ceramic applications.[1)] The Organisation for Economic Co-operation and Development (OECD) Steering Group for Test Guidelines listed nanoparticles as a high-priority group and included cerium oxide nanoparticles in the list along with fullerene, single-walled carbon nanotubes (SWCNTs), multiwalled carbon nanotubes (MWCNTs), silver nanoparticles, and others.

There are some discrepancies regarding the antioxidant/oxidant effects and toxicity of cerium oxide nanoparticles. Several studies have reported that cerium oxide nanoparticles mitigate oxidative stress at a biological level. This antioxidant property of cerium oxide nanoparticles has shown a possibility in the treatment of aging, trauma, and Alzheimer's and Parkinson's diseases.[2–5)] On the other hand,

*To whom correspondence should be addressed: College of Pharmacy, Dongduk Women's University, 23–1 Wolgok-dong, Seongbuk-gu, Seoul 136–714, Republic of Korea. Tel.: +82-2-940-4522; Fax: +82-2-940-4159; E-mail: kspark@dongduk.ac.kr

cerium oxide nanoparticles have also been shown to have toxic effects through the induction of oxidative stress.[1,6,7] The health effects seem to depend on the physicochemical properties of the nanoparticles, such as their surface chemistry, structure, size, preparation methods, exposure concentration, exposure time, and the types of cultured cells used for study.[7,8] In the case of toxicity studies with SWCNTs, discrepancies were also found concerning the effects of SWCNTs on inflammatory responses.[9–11] Although there are still many questions and unresolved problems regarding the toxicity testing of nanomaterials, they have become one of most interesting toxicologic issues in current research.

In this study, we evaluated the pulmonary and systemic inflammatory responses induced in mice by intratracheal instillation of cerium oxide nanoparticles.

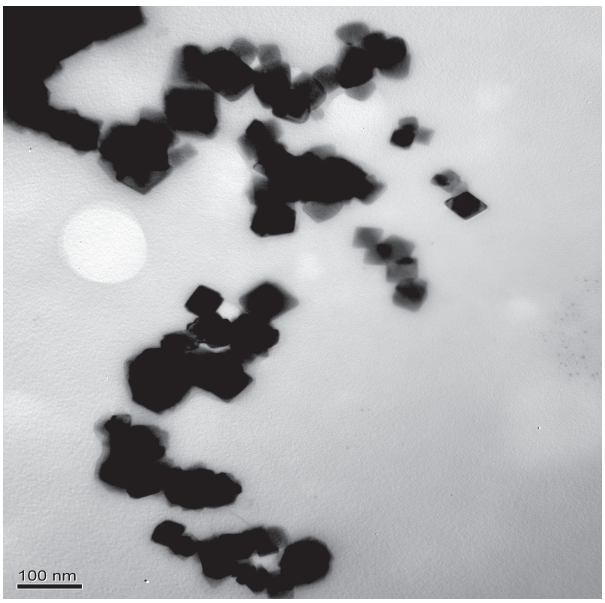

Fig. 1. TEM Image of Cerium Oxide Nanoparticles in PBS

MATERIALS AND METHODS

Preparation of Cerium Oxide Nanoparticles —— Cerium oxide nanoparticles were prepared using the supercritical synthesis method. The synthesis process is outlined as follows. Distilled water, pumped into the system using a high-pressure pump, was heated to a moderate temperature using a heat exchanger and heated further to the desired temperature using a pre-heater. The solution of the metal precursor $Ce(NO_3)_3$ and ammonia water for pH control was pumped into the system using high pressure pumps, and mixed with supercritical water at the mixing point located above the reactor. A sufficient reaction time for the formation of cerium oxide nanoparticles was provided by the reactor to maintain a supercritical condition. The synthesized cerium oxide was collected by a filter, and this was followed by spray drying to obtain the final product. The crystal structure of cerium oxide was confirmed based on the powder X-ray diffraction (XRD) patterns using monochromic Cu-Ka radiation (D/MAX III, Rigaku, Tokyo, Japan). The average crystallite size was also measured using the X-ray line broadening technique employing the Scherrer formula using the profiles of the (1 1 1) peak. Scanning electron microscope (SEM) images of cerium oxide nanoparticles were obtained using a Phillips SEM-535 M microscope operating at an acceleration voltage of 20 kV. The samples were prepared by sprinkling the powder oxides onto double-sided sticky tape and mounting them on a microscope stub. The samples were coated with sputtered gold.[7] Finally, the cerium oxide nanoparticles were suspended in phosphate-buffered saline (PBS, 0.15 M, pH 7.2) and sonicated for 3 min prior to use to ensure a uniform suspension. The average size was about 130 nm because of slight agglomeration. Transmission electron microscope (TEM) images were recorded with a JEM1010 device (JEL, Tokyo, Japan, Fig. 1).

Animals —— ICR male mice (25 ± 1 g) were purchased from Orient-Bio Animal Company (Seongnam, Gyunggi-do, Korea) and were allowed to adapt to the animal room conditions prior to initiation of the study. The environmental conditions were a temperature of 23 ± 1°C, relative humidity of 55 ± 5%, and a 12-hr light/dark cycle. All the animals used in this study were cared for in accordance with the principles outlined in the "Guide for the Care and Use of Laboratory Animals" issued by the Animal Care and Use Committee of the National Veterinary Research and Quarantine Service. The animals were treated to observe dose-dependent ($n = 4$ per group) and time-dependent ($n = 13$ per group) changes, respectively. Body weights were measured weekly from day 0.

Intratracheal Instillation and Sample Preparation —— Cerium oxide nanoparticles were delivered with a 24-gauge catheter at the described dose (dose-dependent change: 50, 100, 200, and 400 mg/kg; time-dependent change: 100 mg/kg) by

intratracheal instillation under light tiletamine anesthesia (day 0). The animals were killed on days 1, 7, 14, and 28 after treatment. In the time-dependent test, samples harvested from four per group were used for cell phenotype change of blood lymphocytes, blood biochemistry, bronchoalveolar lavage (BAL) fluid analysis, nitric oxide (NO) assay in BAL fluid, and gene expression analysis in lung tissue ($n = 4$), and the rest ($n = 9$) was used for cytokine assay and histopathologic analysis. The control group was intratracheally instillated with PBS of the same volume.

At the selected time intervals after instillation, about 1 ml of blood per mouse was collected from the retroorbital venous plexus into heparinized capillary tubes. After centrifugation, 400 μl of serum was obtained from each mouse. BAL fluid collection was performed by cannulating the trachea and lavaging the lungs with 1 ml of cold sterile (Ca^{2+} plus Mg^{2+})-free PBS (0.15 M, pH 7.2). Approximately 500–600 μl of BAL fluid was harvested per mouse, this was centrifuged at 3000 rpm for 10 min, and 400 μl of supernatant per mouse was pooled for cytokine analysis.

To isolate the splenocytes, the spleen was aseptically removed from an ICR mouse and suspended by passage through a sterile plastic strainer in Dulbecco's modified Eagle's medium (DMEM) with 2% fetal bovine serum (FBS). After centrifugation at 1500 rpm for 3 min, the supernatant was discarded, and the pellet was briefly vortexed in 500 μl of distilled water and then resuspended in DMEM with 2% FBS. The cells were filtered through nylon mesh to yield the final splenocyte preparation.[12–14)]

BAL Fluid Analysis —— Total cells in the BAL fluid were quantified by hemocytometric counting, with cell differentials performed on cytocentrifuged preparations fixed in methanol and stained with Diff-Quick (Thermo Shandon, Pittsburgh, PA, U.S.A.). The distribution of alveolar macrophages, neutrophils, and lymphocytes were assessed by their characteristic cell shapes.

Blood Biochemistry —— The sera were stored at the −80°C in a freezer prior to analysis. Total protein, albumin, aspartate aminotransferase (AST), alanine aminotransferase (ALT), alkaline phosphatase (ALP), creatinine, and blood uria nitrogen (BUN) were measured using an autoanalyzer (Hitachi7180, Hitachi, Tokyo, Japan).

Cytokine Measurement —— The concentrations of each cytokine in the supernatant of the BAL fluid and serum were determined using commercially available ELISA kits (eBioscience, San Diego, CA, U.S.A.). Briefly, each well of a microplate was coated with 100 μl of capture antibody and incubated overnight at 4°C. After washing and blocking with assay diluent, BAL fluid, serum, or standard antibody were added to individual wells, and then the plates were maintained for 2 hr at room temperature. The plates were washed, and biotin-conjugated detecting antibody was added to each well and incubated at room temperature for 1 hr. The plates were washed again and further incubated with avidin-horseradish peroxidase for 30 min before detection with tetramethylbenzidine solution. Finally, reactions were stopped by adding H_3PO_4 1 M, and the absorbance at 450 nm was measured with an ELISA reader (Molecular Devices, Sunnyvale, CA, U.S.A.). The amount of cytokine was calculated from the linear portion of the generated standard curve.[13)]

NO Production —— NO production in BAL fluid was quantified spectrophotometrically using the Greiss reagent. The absorbance at 540 nm was measured, and the nitrite concentration was determined using a calibration curve prepared with sodium nitrite as the standard.[15)]

Gene Expression Analysis —— For the preparation of total RNA from lung tissue, the RNAgents total RNA Isolation System (Promega, Madison, WI, U.S.A.) was used according to the manufacturer's instructions. The Reverse-Transcriptase (RT)-PCR reaction was performed with 1 μg of total RNA, 1 μl of 20 μM oligo dT primer, and 18 μl of reaction mixture which was provided by AccuPower RT/PCR PreMix (Bioneer, Daejeon, Korea) at 42° for 60 min. PCR was then carried out in a total of 20 μl for 30 cycles at 95° for 1 min, 55° for 1 min, and 72° for 1 min. Amplified cDNA products were separated on 1.5% agarose gel by electrophoresis. The primer sequences used were: inducible nitric oxide synthase (iNOS); (R)5-AGCTCCTCCCAGGACCACAC; and (L)5-ACGCTGAGTACCTCATTGGC.

Histopathology —— Histopathologic analysis was performed at Biotoxtech (Cheongwon-gun, Chungbuk, Korea), one of the Good Laboratory Practice (GLP) institutes in Korea. Lung tissues were fixed in 10% (v/v) neutral buffered formalin and processed using routine histologic techniques. After paraffin embedding, 3-μm sections were cut and stained with hematoxylin and eosin (H&E) for histopathologic evaluations.

Immunophenotyping —— All monoclonal antibodies were purchased from eBioscience. T cells (CD3, 1 : 50), B cells (CD19, 1 : 50), natural killer (NK) cells (DX5, 1 : 100), $CD4^+$ T cells ($CD4^+$, 1 : 160), and $CD8^+$ T cells ($CD8^+$, 1 : 50) were identified using directly conjugated anti-mouse antibodies. Briefly, splenocytes ($3–5 \times 10^3$ cell/ml) and total blood cells were blocked with Fc-block (eBioscience) to reduce nonspecific antibody binding. Cells were then incubated in the dark with the appropriate fluorochrome-conjugated antibody (10 μl) for 20 min at 4°C. Cells were washed with 500 μl of fluorescence activated cell sorter (FACS) buffer. Red blood cells were then lysed for 5 min with FACS lysis buffer (BD Bioscience, Franklin Lakes, NJ, U.S.A.) at room temperature and rewashed using FACS buffer. Finally, each sample was fixed with 1% paraformaldehyde until analysis. Flow cytometry analysis was performed on the FACSCalibur system (BD Biosciences). Control samples were matched for each fluorochrome. Data were analyzed using CellQuest software (Becton Dickinson, Franklin Lakes, NJ, U.S.A.).[14, 16]

Statistical Analysis —— The values obtained from the control group and the treated groups were compared using Student's *t*-test, and the levels of significance are represented for each result.

RESULTS

Acute Toxicity and Changes in Body Weights after a Single Treatment

For the evaluation of acute toxicity of cerium oxide nanoparticles, high dosages were administered. The animals were not killed by the high dosages used. On day 1, after a single instillation of cerium oxide nanoparticles at doses of 50, 100, 200, and 400 mg/kg, biochemical analysis of mouse serum was performed. No changes in the levels of total protein, albumin, or cholesterol were observed in response to cerium oxide nanoparticles instillation (data not shown).

Mice treated with cerium oxide nanoparticles at 100 mg/kg showed slightly decreased body weight on day 1 after instillation (Fig. 2), but this was not a statistically significant difference. Decreased consumption of diet may have been the reason for the body weight decrease on day 1 after instillation. No growth inhibition in response to cerium oxide nanoparticle administration was observed over the duration of the experiment until day 14 after instillation.

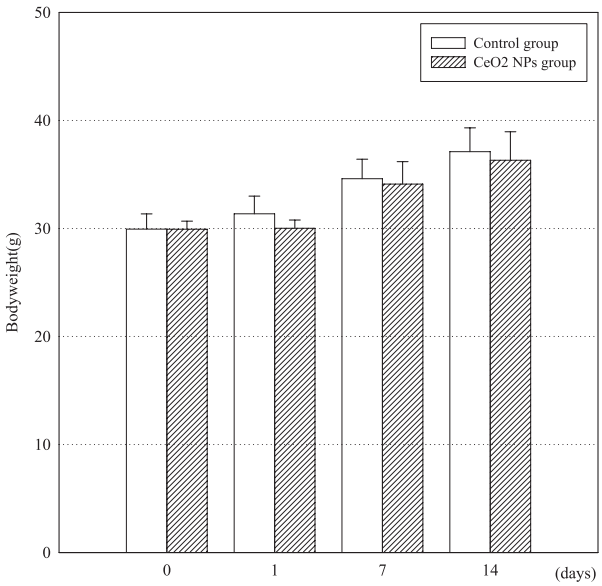

Fig. 2. Body Weight Changes of Mice after Instillation of Cerium Oxide Nanoparticles (n = 13)

Body weights were measured on days 0, 1, 7, and 14 after instillation of cerium oxide nanoparticles (100 mg/kg). Day 0 designates the day of instillation.

Dose-Dependent Induction of Cytokines in BAL Fluid

When mice were treated with increasing doses of cerium oxide nanoparticles, interleukin (IL)-6 and IL-12 were induced in BAL fluid in a dose-dependent manner (Fig. 3). IL-6 was maximally induced at a nanoparticle dose of 100 mg/kg, followed by a decrease at higher dosages. In the case of IL-12, maximal induction was shown at 200 mg/kg, followed by a decline with further increases in dosage. Based on these dose-response results, a 100 mg/kg dosage of cerium oxide nanoparticles was used in all further studies.

Cell Distribution in BAL Fluid

The number of total cells recovered in BAL fluid from mice treated with cerium oxide nanoparticles, was not significantly increased on day 1 after instillation but significantly increased by day 14 (Fig. 4A). On day 7, a slight increase in cell number was evident but was not statistically significant. When the composition of cells in BAL fluid was analyzed, the percentage composition of BAL-recovered neutrophils, which are characteristic of the initial stage of inflammation, was maximally increased on day 1 following instillation. The distribution of neutrophils then gradually decreased over

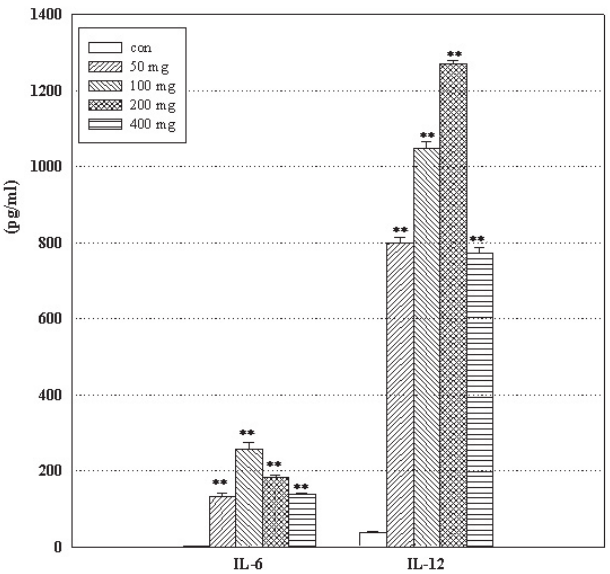

Fig. 3. Changes in IL-6 and IL-12 Levels in BAL Fluid after Instillation of Cerium Oxide Nanoparticles ($n = 4$)

Mice were instilled intratracheally with cerium oxide nanoparticles at the dose of 50, 100, 200, or 400 mg/kg per day and killed on day 1 after instillation. **Significantly different from control group, $p < 0.01$.

the remainder of the experimental period. The distribution ratio of macrophages was different from that of neutrophils, as a significant decrease was seen on day 1 after instillation. The distribution ratio of lymphocytes was not changed on day 1 after instillation, but increased to 3.5-fold of the control level by day 14 (Fig. 4B).

Time-Dependent Induction of Cytokines in BAL Fluid

The concentrations of proinflammatory cytokines including IL-1, IL-6, tumor necrosis factor (TNF)-α, Th1-type cytokines [IL-12 and interferon (IFN)-γ], and Th2-type cytokines (IL-4, IL-5, and IL-10) were measured in BAL fluid harvested at different times after intratracheal instillation (Table 1). The proinflammatory cytokines (IL-1, TNF-α, and IL-6) were significantly increased on day 1 after instillation. In the case of IL-6 and TNF-α, the elevated levels on day 1 were decreased on days 7, 14, and 28 after instillation. However, IL-1 was sustained at an elevated level until day 28 after instillation. The levels of Th2-type cytokines such as IL-4, IL-5, and IL-10 were also significantly elevated to 9.77, 7.72, and 129.08 pg/ml, respectively, on day 1 after instillation. These also decreased over the remainder of the experimental period. IL-12 and IFN-γ, which are Th1-type cytokines, were also significantly increased to 1047.95 and 13.85 pg/ml, respectively. After significant increases in all the cytokines measured on day 1 after instillation, the levels gradually decreased but were still significantly higher than the initial control levels, even on day 28 after instillation.

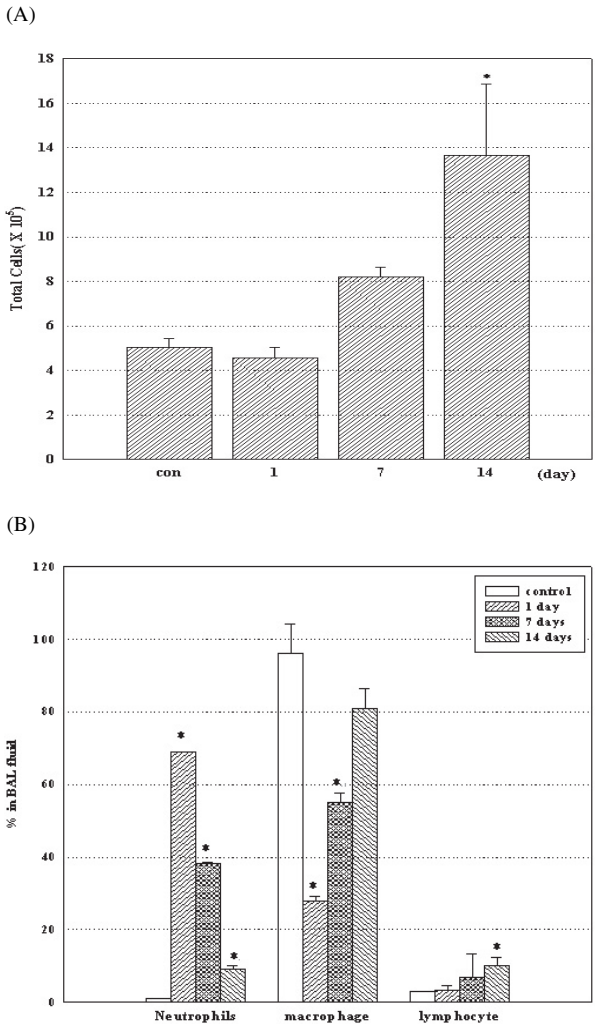

Fig. 4. Changes in Cell Distribution in BAL Fluid after Instillation of Cerium Oxide Nanoparticles ($n = 4$)

Mice were instilled with cerium oxide nanoparticles 100 mg/kg and then killed on the designated days (1, 7, and 14). Total cells in BAL fluid were quantified by hemocytometric counting (A), and the distribution of alveolar macrophages, neutrophils, and lymphocytes was determined based on the characteristic cell shapes (B). *Significantly different from control group, $p < 0.05$.

Time-Dependent Induction of Cytokines in Blood

The possibility of instilled cerium oxide nanoparticles inducing systemic inflammatory responses was estimated by measuring the levels of cytokines in the blood. As shown in Fig. 5, the levels of all measured cytokines, except for IL-1,

Table 1. Changes in Cytokine Levels in BAL Fluid with Time after Instillation of Cerium Oxide Nanoparticles

Mice were instilled with cerium oxide nanoparticles 100 mg/kg and killed on the designated days (1, 7, 14, and 28). BAL fluid collected from 3 mice were pooled, and three separate samples were prepared from 9 mice per group. *,**Significantly different from control group, $p < 0.05$ and $p < 0.01$, respectively.

	control	Day 1	Day 7	Day 14	Day 28
IL-1	2.85 ± 0.45	12.39 ± 2.11**	10.49 ± 0.19**	9.77 ± 1.62**	6.18 ± 0.46**
TNF-α	3.00 ± 0.60	163.32 ± 2.44**	33.74 ± 1.60**	21.54 ± 2.33**	10.21 ± 0.35*
IL-6	1.40 ± 0.72	256.94 ± 19.08**	20.76 ± 0.59**	16.12 ± 1.22**	7.93 ± 1.61*
IL-4	1.22 ± 0.48	9.77 ± 0.73**	8.60 ± 0.65**	6.48 ± 0.25**	5.29 ± 0.00**
IL-5	1.11 ± 0.11	7.72 ± 0.24**	4.70 ± 0.12**	3.92 ± 0.23**	2.10 ± 0.21*
IL-10	18.34 ± 5.59	129.08 ± 9.58**	110.51 ± 7.84**	49.59 ± 5.59**	45.52 ± 5.48*
IL-12	9.15 ± 1.36	1047.95 ± 124.91**	616.44 ± 73.77**	236.87 ± 5.87**	149.51 ± 1.51**
IFN-γ	1.00 ± 0.13	13.85 ± 0.17**	10.21 ± 0.21**	6.08 ± 0.48**	2.68 ± 0.33*

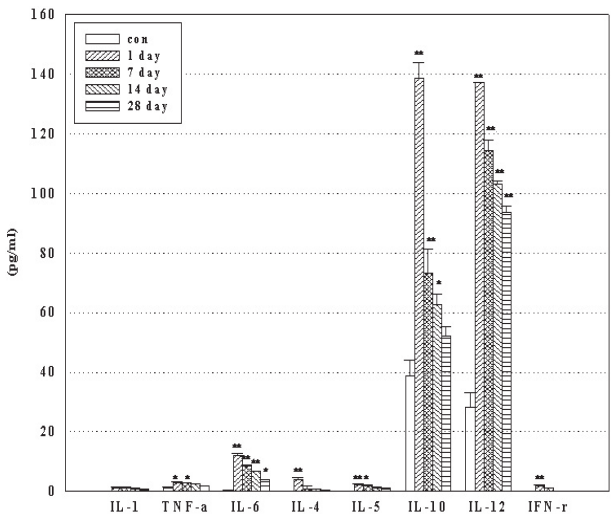

Fig. 5. Changes in Cytokine Levels in Serum with Time after Instillation of Cerium Oxide Nanoparticles

Mice were instilled with cerium oxide nanoparticles at 100 mg/kg and killed on the designated days (1, 7, 14, and 28). Blood collected from 3 mice were pooled, and three separate samples were prepared from 9 mice per group. *,**Significantly different from control group, $p < 0.05$ and $p < 0.01$, respectively.

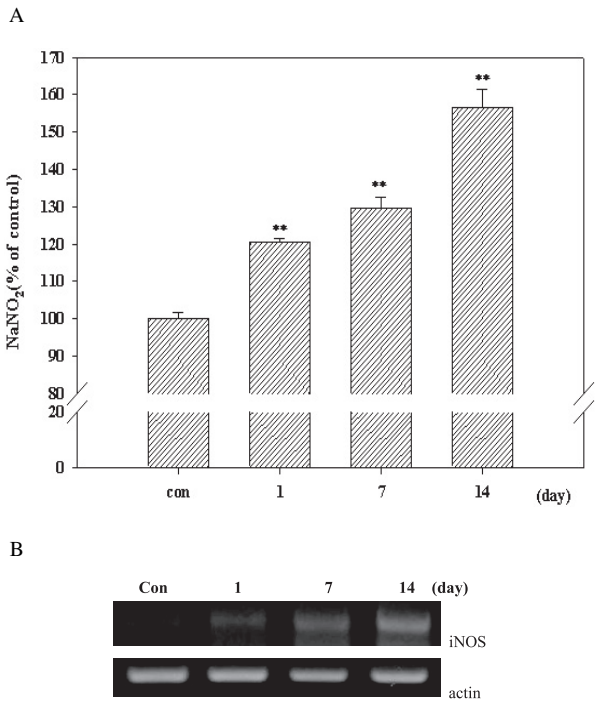

Fig. 6. Increase in NO Level and Gene Expression of iNOS with Time after Instillation of Cerium Oxide Nanoparticles ($n = 4$)

Mice were instilled with cerium oxide nanoparticles 100 mg/kg and killed on the designated days (1, 7, and 14) (A). **Significantly different from control group, $p < 0.01$. mRNA transcription was detected by RT-PCR analysis and the results were confirmed by several individual replicate experiments. A representative image is shown (B).

were significantly increased in the blood samples. A maximal increase was seen on day 1 after instillation and the elevated levels gradually declined with time. When the induction levels were compared to those in BAL fluid, the levels of cytokines induced in the blood were relatively lower than those in BAL fluid.

NO Generation

The concentration of NO, a proinflammatory molecule, was elevated in BAL fluid after cerium oxide nanoparticle instillation. The level in the control group BAL was $1.16 \pm 0.05\,\mu M$ and this increased after instillation of nanoparticles in a time-dependent manner. The maximal level, which was about 160% of the control level, occurred on day 14 after instillation (Fig. 6A). Gene expression of iNOS showed a similarly time-course pattern for NO synthesis (Fig. 6B).

Histopathology of the Lung

Representative lung sections at each time point are shown in Fig. 7. On day 1 after instillation, cerium oxide nanoparticles were observed primar-

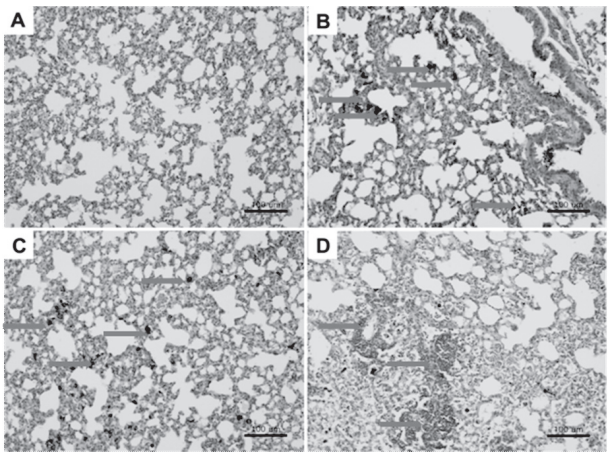

Fig. 7. Histopathologic Changes in Lung Tissues after Instillation of Cerium Oxide Nanoparticles

Mice were instilled with cerium oxide nanoparticles 100 mg/kg and killed on the designated days (1, 7, and 14). Nine lung tissue samples were examined per group. A representative image is shown (original magnification ×200). A, vehicle control mice; B, Image of day 1 (arrows show aggregated nanoparticles); C, image on day 7 (arrows show aggregated nanoparticles); D, image on day 14 (arrows show granuloma region).

ily in the alveoli, bronchiole, and bronchoalveolar junction (Fig. 7B). On day 7 after instillation, nanoparticles were also observed in the alveolar macrophages or the interstitial regions of alveolar septa (Fig. 7C). The inflammatory reaction of granuloma formation was not observed until 7 days after instillation. However, granuloma with lymphocytes, which are known to indicate chronic inflammation, were observed on day 14 after instillation (Fig. 7D). Nontreated control lung tissue is shown in Fig. 7A.

Lymphocyte Phenotypes

The instillation of cerium oxide nanoparticles induced changes in cell phenotype (Fig. 8A). While B and T cells of accounted for 71.3% and 23.0%, respectively, of the control cell types, the distribution of B and T cells in splenocytes of mice treated with cerium oxide nanoparticles was changed to 54.7/40.4%, 54.8/40.3%, and 53.8/41.9% on day 1, 7, and 14 after instillation, respectively. This change was also observed in blood lymphocytes (data not shown). The ratio of $CD4^+$ T cells to $CD8^+$ T cells, which are subtypes of T cells, changed from 3-fold to 3.5-, 4.4-, and 4.4-fold on days 1, 7, and 14 after instillation, respectively (Fig. 8B).

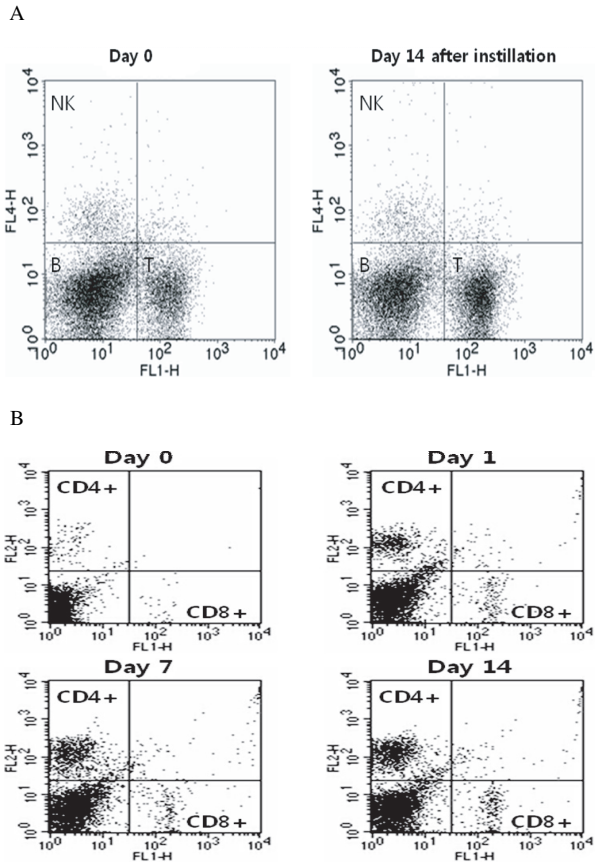

Fig. 8. Cell Distribution of Lymphocytes after Instillation of Cerium Oxide Nanoparticles ($n = 4$)

Mice were instilled with cerium oxide nanoparticles 100 mg/kg and were killed on the designated days (1, 7, and 14). Results were confirmed by several individual replicate experiments. A representative image is shown. (A) Cell distribution in splenocytes of the control group and day 14 group. (B) Distribution of T cell subtype in splenocytes of the control and treated groups (days 1, 7, and 14).

DISCUSSION

In recent years, cerium oxide nanoparticles have attracted much attention as a fine UV absorbent and high-activity catalyst.[17] Some reports also suggested that these have potential as nanomedicines due to their possible scavenging effects on reactive oxygen species (ROS).[18] However, some discrepancies exist for the ROS-scavenging capabilities of cerium oxide nanoparticles.[7] These discrepancies might result from differences in surface chemistry, size, dose, exposure time, and other test systems. Cerium ion may exist as Ce^{3+} or Ce^{4+} in solution, and it is known that Ce^{3+} acts as a radical scavenger, while Ce^{4+} acts as a radical generator.[5] However, no direct evidence has shown that cerium oxide nanoparticles exist in an ionic state (Ce^{3+} or Ce^{4+}) in target cells. Therefore the different biolog-

ical effects of cerium oxide nanoparticles cannot be reasonably explained by the Ce^{3+} or Ce^{4+} ionic state of cerium. With the nature of cerium nanoparticle toxicity unclear, the applications of cerium nanoparticles raise issues concerning their potential human health risk. In this study, we investigated the proinflammatory effects of cerium oxide nanoparticles based on our previous report on the induction of oxidative stress.[7)]

As shown in Fig. 1, cerium oxide nanoparticles suspended in PBS for intratracheal instillation were agglomerated and the mean diameter of agglomerated particles was 134 nm, which means the agglomerated particles are nano-sized, not micro-sized. Although cerium oxide nanoparticles were agglomerated in solution like many other nanoparticles, the agglomerated particles were stable after sonification and the nano-size was not changed to micro-size agglomerates prior to instillation. When mice were treated with cerium oxide nanoparticles by intratracheal instillation, phagocytosis by alveolar macrophages was observed (data not shown), and innate immune responses were triggered. Proinflammatory cytokines including IL-1, TNF-α, and IL-6, and chemokines such as IL-8 released by macrophages were involved in the first stage of this process. The levels of IL-1, IL-6, and TNF-α in BAL fluid were significantly increased on day 1 after instillation. The increased ratio of IL-1, TNF-α, and IL-6 in BAL fluid was 4.4-, 54.4-, and 183.5-fold the control level, respectively. Similar changes were also observed in previous studies using silica nanoparticles, SWCNTs, and TiO_2 rods and dots.[11, 19, 20)] Regarding the dose of instilled nanoparticles and proinflammatory responses, various ranges were used. When SWCNTs were intratracheally instilled in rats at a dose of 5 mg/kg, the number of total cells in BAL fluid was not increased.[20)] It was reported that BAL levels of TNF-α were significantly increased in rats treated with MWCNTs 2 mg/animal.[21)] In the case of cerium oxide nanoparticles, the dosages used in this study were relatively higher than those of carbon nanotubes. However, cerium oxide nanoparticles may cause inflammatory responses at lower doses than used in this study because the increases in IL-6 and IL-12 by cerium oxide nanoparticles 50 mg/kg were so extraordinary (Fig. 3).

The activation and increased levels of cytokines were followed by an increase in neutrophil number in BAL fluid (Fig. 4B). The distribution ratio of neutrophils in BAL fluid was increased to 68.8% on day 1 after instillation.

Activated macrophages also stimulated naive T cells to trigger adaptive immune system responses. T cells can be subdivided into two populations according to their expression of $CD4^+$ or $CD8^+$ molecules. In normal human peripheral blood, the contribution ratio of $CD4^+$ T cells and $CD8^+$ T cells is approximately 2 : 1, but this may be significantly altered by immunodeficiency diseases, autoimmune diseases, and other disorders. Furthermore, $CD4^+$ T cells differentiate to Th1 cells by Th1-type cytokines, such as IL-12, and to Th2 cells by Th2-type cytokines such as IL-10. Th1 cells can secrete various cytokines including as IFN-γ and IL-12. As shown in Table 1, IFN-γ and IL-12 were significantly induced by cerium oxide nanoparticles and these cytokines activated Th-1 cells. Thus cerium oxide nanoparticles may activate alveolar macrophages to stimulate innate immune responses and to trigger cell-mediated inflammatory responses through the activation of NK cells or macrophages. Furthermore, cerium oxide nanoparticles also induced Th2-type cytokines such as IL-4, IL-5, and IL-10 in BAL fluid, which may trigger allergic responses by the activation of B cells.

In this study, the number of $CD4^+$ T cells was significantly increased compared with the number of $CD8^+$ T cells on day 1 after instillation (Fig. 8B). This change was maintained over the remainder of the experimental period until day 14 after instillation. When we compared the increased level of IL-10 (Th2-type cytokine) and IL-12 (Th1-type cytokine) in BAL fluid, IL-12 showed a greater response to the cerium oxide nanoparticles than did IL-10. IL-10 was increased by 11.5-fold, while IL-12 was increased by as much as 115.2-fold of the control level on day 1 after instillation (Table 1). IFN-γ, also a Th1-type cytokine, was increased by 13.9-fold of the control level in BAL fluid on day 1 after instillation.

Regarding the Th2-type cytokines, IL-4 induces $CD4^+$ T cells to differentiate into Th2 cells, and these activated Th2 cells may activate B cells to produce IgE. IL-5 also promotes the synthesis of antibodies, both IgE and IgG2. In this study, IL-4 and IL-5 of Th2-type cytokines were increased to 8- and 7.7-fold, respectively, of the control level in BAL fluid on day 1 after instillation. Although both Th1- and Th2-type cytokines were simultaneously increased, the Th1-type cytokines were more responsive to cerium oxide nanoparticles than were Th2-type cytokines, as shown in Table 1.

Th1 and Th2 cells have very different functions. Th2 cells are the most effective activators of B cells, especially in primary responses, whereas Th1 cells are crucial for activating macrophages and function in delayed-type hypersensitivity. However, under many circumstances *in vivo*, there are mixed Th1 and Th2 responses, and the overall effects are determined by the dominant response. In this study, Th1 responses seemed to be more dominant than Th2 responses, which suggests that cerium oxide nanoparticle instillation may favor induction of delayed-type hypersensitivity.

As shown in Table 1 and Fig. 5, cytokines measured in BAL fluid and blood were decreased following an initial rapid increase on day 1 after instillation. However, the induction of NO and the gene expressions of iNOS in lung tissue (Fig. 6) increased in a time-dependent manner until day 14 after instillation, when granuloma formation was observed (Fig. 7D). Elevated gene expression of cyclooxygenase-2 and IL-5 was also maintained until day 14 after instillation (data not shown). This may have been caused by nanoparticles that physically translocated from the instilled bronchus into the lung tissue, where they were retained for a long time, causing inflammatory responses such as granuloma and/or fibrosis through persistent damage to the lung.

In summary, cerium oxide nanoparticles may induce delayed-type hypersensitivity through the induction of proinflammatory cytokines, predominantly by Th1 responses. In addition, they may also cause granuloma or fibrosis in the lungs of mice after intratracheal instillation.

Acknowledgement This work was supported by the Ministry of Environment Eco-technopia 21 project.

REFERENCES

1) Lin, W., Huang, Y. W., Zhou, X. D. and Ma, Y. (2006) Toxicity of cerium oxide nanoparticles in human lung cancer cells. *Int. J. Toxicol.*, **25**, 451–457.
2) Schubert, D., Dargusch, R., Raitano, J. and Chan, S. W. (2006) Cerium and yttrium oxide nanoparticles are neuroprotective. *Biochem. Biophys. Res. Commun.*, **342**, 86–91.
3) Singh, N., Cohen, C. A. and Rzigalinski, B. A. (2007) Treatment of neurodegenerative disorders with radical nanomedicine. *Ann. N.Y. Acad. Sci.*, **1122**, 219–230.
4) Niu, J., Azfer, A., Rogers, L. M., Wang, X. and Kolattukudy, P. E. (2007) Cardioprotective effects of cerium oxide nanoparticles in a transgenic murine model of cardiomyopathy. *Cardiovasc. Res.*, **73**, 549–559.
5) Das, M., Patil, S., Bhargava, N., Kang, J. F., Riedel, L. M., Seal, S. and Hickman, J. J. (2007) Autocatalytic ceria nanoparticles offer neuroprotection to adult rat spinal cord neurons. *Biomaterials*, **28**, 1918–1925.
6) Thill, A., Zeyons, O., Spalla, O., Chauvat, F., Rose, J., Auffan, M. and Flank, A. M. (2006) Cytotoxicity of CeO_2 nanoparticles for *Escherichia coli*. Physicochemical insight of the cytotoxicity mechanism. *Environ. Sci. Technol*, **40**, 6151–6156.
7) Park, E. J., Choi, J., Park, Y. K. and Park, K. (2008) Oxidative stress induced by cerium oxide nanoparticles in cultured BEAS-2B cells. *Toxicology*, **245**, 90–100.
8) Lison, D. and Muller, J. (2008) Lung and systemic responses to carbon nanotubes (CNT) in mice. *Toxicol. Sci.*, **101**, 179–180.
9) Murr, L. E., Garza, K. M., Soto, K. F., Carasco, A., Powell, T. G., Ramirez, D. A., Guerrero, P. A., Lopez, D. A. and Venzor, J., III. (2005) Cytotoxicity assessment of some carbon nanotubes and related carbon nanoparticle aggregates and the implications for anthropogenic carbon nanotube aggregates in the environment. *Int. J. Environ. Res. Public Health*, **2**, 31–42.
10) Mitchell, L. A., Gao, J., Wal, R. V., Gigliotti, A., Burchiel, S. W. and McDonald, J. D. (2007) Pulmonary and systemic immune response to inhaled multiwalled carbon nanotubes. *Toxicol. Sci.*, **100**, 203–214.
11) Chou, C. C., Hsiao, H. Y., Hong, Q. S., Chen, C. H., Peng, Y. W., Chen, H. W. and Yang, P. C. (2008) Single-walled carbon nanotubes can induce pulmonary injury in mouse model. *Nano Lett.*, **8**, 437–445.
12) Manosroi, A., Saraphanchotiwitthaya, A. and Manosroi, J. (2005) In vitro immunomodulatory effect of Pouteria cambodiana (Pierre ex Dubard) Baehni extract. *J. Ethnopharmacol.*, **101**, 90–94.
13) Byun, J. A., Ryu, M. H. and Lee, J. K. (2006) The immunomodulatory effects of 3-monochloro-1,2-propanediol on murine splenocyte and peritoneal macrophage function in vitro. *Toxicol. in Vitro*, **20**, 272–278.
14) Vendrame, M., Gemma, C., Pennypacker, K. R., Bickford, P. C., Sanberg, D. C., Sanberg, P. R. and Willing, A. E. (2006) Cord blood rescues stroke-

induced changes in splenocyte phenotype and function. *Exp. Neurol.*, **199**, 191–200.

15) Chen, F., Sun, S. C., Kuh, D. C., Gaydos, L. J. and Demers, L. M. (1995) Essential role of NF-κB activation in silica-induced inflammatory mediator production in macrophages. *Biochem. Biophys. Res. Commun.*, **214**, 985–992.
16) Silva, I. A., Graber, J., Nyland, J. F. and Silbergeld, E. K. (2005) In vitro $HgCl_2$ exposure of immune cells at different stages of maturation: effects on phenotype and function. *Environ. Res.*, **98**, 341–348.
17) Yin, L., Wang, Y., Pang, G., Koltypin, Y. and Gedanken, A. (2002) Sonochemical synthesis of cerium oxide nanoparticles effect of additives and quantum size effect. *J. Colloid Interface Sci.*, **246**, 78–84.
18) Gilmore, J. L., Yi, X., Quan, L. and Kabanov, A. V. (2008) Novel nanomaterials for clinical neuroscience. *J. Neuroimmunol. Pharmacol.*, **3**, 83–94.
19) Cho, W. S., Choi, M., Han, B. S., Cho, M., Oh, J., Park, K., Kim, S. J., Kim, S. H. and Jeong, J. (2007) Inflammatory mediators induced by intratracheal instillation of ultrafine amorphous silica particles. *Toxicol. Lett.*, **175**, 24–33.
20) Warheit, D. B., Laurence, B. R., Reed, K. L., Roach, D. H., Reynolds, G. A. and Webb, T. R. (2004) Comparative pulmonary toxicity assessment of single-wall carbon nanotubes in rats. *Toxicol. Sci.*, **77**, 117–125.
21) Muller, J., Huaux, F., Moreau, N., Mission, P., Heilier, J., Delos, M., Arras, M., Fonseca, A., Nagy, J. B. and Lison, D. (2005) Respiratory toxicity of multi-wall carbon nanotubes. *Toxicol. Appl. Pharmcol.*, **207**, 221–231.